

Clustering in ^{13}C

Luka Palada^{1,*}, Neven Soić¹, Louis Acosta², Sam Bailey³, Daniele Dell'Aquila^{4,5}, Jose Antonio Duenas⁶, Juan Pablo Fernandez-Garcia⁷, Pierpaolo Figuera⁸, Enrico Fioretto⁹, Maria Fisichella⁸, Laura Grassi¹, Oliver Kirsebom¹⁰, Tzany Kokalova Wheldon³, Marcello Lattuada⁸, Gloria Marquinez-Duran¹¹, Ismael Martel¹¹, Tea Mijatović¹, Lovro Prepolec¹, Natko Skukan¹, Robin Smith¹², Suzana Szilner¹, Vedrana Tokić¹, Milivoj Uroić¹, Nikola Vukman^{1,13}, Joe Walshe³, and Carl Wheldon³

¹Institut Ruđer Bošković, Zagreb, Croatia

²Instituto de Física, Universidad Nacional Autónoma de México, México City, México

³School of Physics and Astronomy, University of Birmingham, Birmingham, United Kingdom

⁴Dipartimento di Fisica "Ettore Pancini", Università degli Studi di Napoli "Federico II", Napoli, Italy

⁵INFN Sezione di Napoli, Naples, Italy

⁶Departamento de Ingeniería Eléctrica y Centro de Estudios Avanzados en Física, Matemáticas y Computación (CEAFMC), Universidad de Huelva, Huelva, Spain

⁷Departamento FAMN, Universidad de Sevilla, Sevilla, Spain

⁸INFN Laboratori Nazionali del Sud, Catania, Italy

⁹INFN Laboratori Nazionali di Legnaro, Legnaro, Italy

¹⁰Department of Physics and Astronomy, Aarhus University, Aarhus, Denmark

¹¹Departamento de Ciencias Integradas, Universidad de Huelva, Huelva, Spain

¹²Department of Engineering and Mathematics, Sheffield Hallam University, Sheffield, United Kingdom

¹³Department of Physics, University of Split, Faculty of Science, Split, Croatia

Abstract. Measurement was conducted at the INFN-LNL, employing a Tandem accelerator to achieve a 95 MeV ^{14}N beam focused on ^{10}B target ($201 \mu\text{g}/\text{cm}^2$) with the aim to explore the cluster structures of light carbon isotopes. The main focus of this report will be on the ^{13}C nucleus. Data were collected with a six-telescope detection system that allowed for the observation of many-body exit channels. Here are presented some results of the data analysis for the excited states of ^{13}C from reactions with two and three products in the exit channel. In the $^{10}\text{B}(^{14}\text{N},^{11}\text{C})^{13}\text{C}$ reaction, well-defined peaks were identified at 2.0, 3.7, 5.7, 7.4, 9.4, 11.7, 13.9, and 15.9 MeV. The states from ground state to 5.7 MeV are well understood and are used to correct the spectrum, while more states can contribute to the states at higher excitations and further investigation is needed. In the $^{10}\text{B}(^{14}\text{N},^{11}\text{C}^9\text{Be})^4\text{He}$ channel, states were identified at 13.1, 13.9, 15.6, and 18.5 MeV. The experimental results show consistency with the previously published data, supporting theoretical models of clustering and molecular-like structures in ^{13}C . Further analysis of other reaction channels and states will be presented in future publications, aiming to enhance our understanding of multi-center clustering in carbon isotopes.

1 Introduction

The studies of the structure of light nuclei, particularly carbon isotopes, have long been of interest due to their potential for complex configurations, including cluster and molecular-like states. Among these, the ^{13}C nucleus stands out as a key system for exploring how the addition of a single neutron affects the well-established three-alpha (3α) cluster structure of ^{12}C . Understanding the structure of ^{13}C is essential for evaluating the effects of valence neutrons on nuclear clustering, which has broader implications for nuclear theory and the understanding of fundamental interactions in light nuclei.

In the case of ^{12}C , the Hoyle state at 7.65 MeV, having a well-known 3α -cluster configuration and being a crucial state in stellar nucleosynthesis enhancing the 3α fusion

process, has been thoroughly studied. Its structure has been linked to many different configurations: from gas-like configurations and Bose-Einstein condensation [1–5] to linear chain-like [6, 7] arrangements of alpha particles. Extending these concepts to ^{13}C , which incorporates an extra neutron, opens new ways for exploring the stabilization of exotic nuclear structures and molecular configurations. Theoretical models such as Antisymmetrized Molecular Dynamics (AMD) [8], the Generator Coordinate Method (GCM) [9], and the Orthogonality Condition Model (OCM) [10] have been employed to predict the structural properties of ^{13}C . These models suggest that ^{13}C may show states analogous to the Hoyle state of ^{12}C .

The ^{13}C nucleus has also been the focus of recent investigations due to its potential for supporting more complex cluster arrangements, including both bent and linear-chain configurations. The extra neutron in ^{12}C is theorized

*e-mail: luka.palada@irb.hr

[11] to play a stabilizing role in these systems, analogous to molecular bonding in atomic systems. Neutrons are thought to act as covalent bonds between alpha clusters, which has already been observed in neutron-rich beryllium isotopes [12–15]. In ^{13}C , similar molecular states are expected, with the neutron binding together the three alpha cores to form a more stable structure. These configurations give rise to rotational bands of states with distinct energy levels and angular momenta [16], some of which have been theoretically calculated [9] and already identified [17–20]. Specifically, rotational bands in ^{13}C , built upon its $3/2^-$ state at 9.897 MeV, are thought to represent a bent linear-chain arrangement of three alpha clusters with a valence neutron. The presence of large moments of inertia in these bands indicates highly deformed, possibly molecular-like structures, which are consistent with theoretical predictions of rotational bands near the $3\alpha+n$ threshold.

Experimental attempts to validate these theoretical predictions have utilized reactions such as $\alpha+^9\text{Be}$ elastic and inelastic scattering [17, 18], different transfer reactions [21–23], and ^{13}C inelastic scattering [20, 24, 25] to probe the high-energy structure of ^{13}C . These experiments aim to clarify the spin-parity assignments and molecular characteristics of states at excitation energies above the alpha emission threshold (10.648 MeV). While significant progress has been made, conflicting experimental results especially regarding spin parity assignments and lack of high-precision data at higher energies continue to limit our understanding of ^{13}C 's structure. Further experimental and theoretical investigations are necessary to fully understand the rich structure of ^{13}C and its implications for broader nuclear physics.

2 Experiment and analysis

The experiment was carried out at the INFN-LNL in Legnaro, focusing on studying clustering in carbon and other light nuclei isotopes. Nuclear reactions were induced by accelerating a beam of ^{14}N to 95 MeV on many targets, with most of them containing ^{10}B . Most of the collected experimental data was with $201 \mu\text{g}/\text{cm}^2$ ^{10}B target with a thin formvar backing. Thin gold target was used for calibration purposes alongside a triple-alpha source enabling good calibration throughout the whole energy range.

Since the main interest of the experiment is the cluster structure and a strong indication of that structure is the detection of the cluster decay products (see, for example, [13–15, 26, 27]), the detector system was set up as shown on the figure 1, with three detectors on each side of the beamline. In this way, a wide range of angles was covered (from 15° to 72°) and it was possible to detect many decay products since most of the interesting data came from the events with three or four reaction products in the exit channel.

The detection system employed six telescopes, each equipped with a thick double-sided E detector ($4 \times 1000 \mu\text{m}$ and $2 \times 500 \mu\text{m}$) and a thin single-sided ΔE detector ($6 \times 20 \mu\text{m}$). The E detector had strips on both sides, creating a grid of 256 pixels, while the ΔE detector was single-

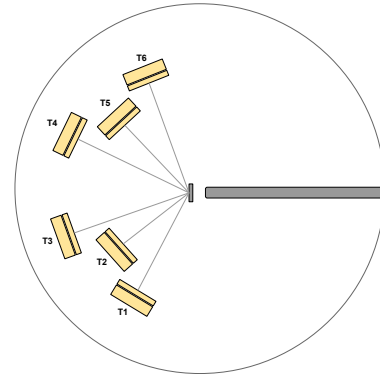


Figure 1: Detector setup showing the position of six telescope detectors inside the chamber with three on each side of the beamline covering from 15° to 72° .

sided. The segmentation of the detectors allowed for precise detection angles determination, with each pixel accounting for up to one degree.

The identification of reaction products was carried out using the standard ΔE -E method, where the energy deposited in the E detector is plotted against the energy lost in the ΔE detector, as illustrated in Figure 2. This method allowed for the clear separation of various isotopes, ranging from helium to oxygen. Then, the ΔE -E spectra were processed using a semi-automated approach with a multi-parameter function [28, 29], enabling the identification of various isotopes by applying one-dimensional cuts.

During the experiment, both single-hit and coincidence data were gathered to examine reaction exit channels involving two, three, or more reaction products, where in each case only one of the reaction products could go undetected. In this way, knowing detection energy and geometry, the event's full kinematics could be reconstructed, allowing for the determination of the excitation energy of the observed state. To reduce systematic errors from factors such as nonuniformity of the ΔE detectors, uncertainties in the detector geometry, and inaccuracies in energy-loss calculations, all possible combinations of detected reaction products were analyzed separately for different telescope combinations. Finally, adjustments were made to account for energy loss in the detector's dead layers.

Although single-hit data provided some insights into the cluster structure, the main emphasis here is on coincidence data from many-body reactions. Because the majority of the analyzed data involve such reactions, a brief overview of the analysis procedure for these types of events will be outlined here.

In the case of single detection events missing mass method was applied and excitation energy was calculated according to the expression:

$$\begin{aligned}
 E_x &= E_a + Q_0 - E_b - E_B = \\
 &= Q_0 + \frac{M_B - M_a}{M_B} E_a - \frac{M_B + m_b}{M_B} E_b \\
 &+ \frac{2}{M_B} \sqrt{M_A M_B E_a E_b} \cos \theta_b, \quad (1)
 \end{aligned}$$

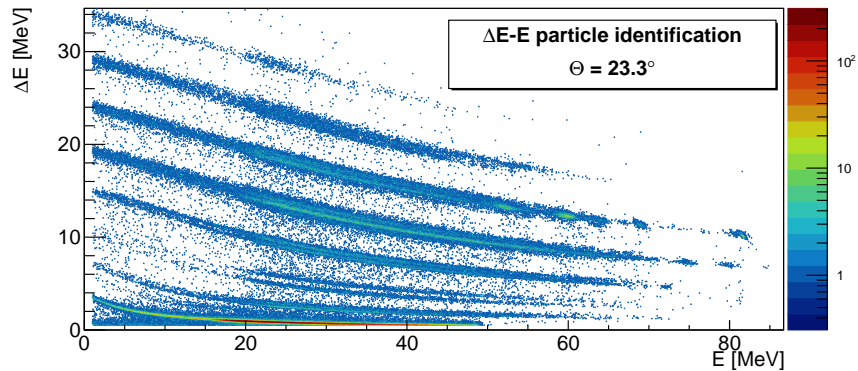


Figure 2: Typical example of the particle identification spectrum obtained with the silicon strip detector telescopes for one pixel at the polar angle of 23.3° .

where a represents the projectile, A the target, b the detected product, and B the undetected product. Data with two products in the exit channel was also used to test and correct the estimated detector geometry by plotting spectra of excitation energy versus detected angles and checking the identification of the reaction channel, as we'll see in the next section.

For the analysis of the reactions with three products in the exit channel example is given on the $^{10}\text{B}(^{14}\text{N}, ^{11}\text{C}^9\text{Be})^4\text{He}$ exit channel. Since two out of three products are detected, to be able to continue with the analysis it is important to choose the data that corresponds to the reaction of interest, i.e. the data with the third undetected product being one from the reaction. Correlation plot, so-called Catania plot [30], was used to identify the third product and to determine the missing energy in the exit channel. The missing energy and momentum of the third product were calculated, and new variables were plotted for each event on the Catania plot, resulting in loci that differ based on slope and y-axis intersection. The slope provides the mass of the undetected particle, while the y-axis intersection yields the Q value of the reaction. Combining the Catania plot with Q -value spectra projections enabled event cuts that identified the exit channel. Catania plot and Q -value spectrum for this reaction, where the ^4He was undetected are displayed in Figure 3. The observed loci slopes confirm the undetected particle's mass as $A = 4$, thus validating the reaction channel identification. Four separate loci are visible (four lines on the Q spectra), with the lowest one (furthest right) representing the ground state, the one above (second from the right) indicating the ^{11}C first excited state at 2 ($1/2^-$) MeV, and the last two (last two on the left) representing what could possibly be a mixture of more than one state in ^{11}C .

Specific for this type of reactions when there are more than two products in the exit channel is that products can be the result of the decay of different intermediate states. For example, products in $^{10}\text{B}(^{14}\text{N}, ^{11}\text{C}^9\text{Be})^4\text{He}$ reaction could have resulted from the decay of ^{13}C , ^{15}O , or ^{20}Ne . To exclude the events from intermediate states that contaminate the data, correlation plots between excitation energies of different product combinations were plotted in Figure 6.

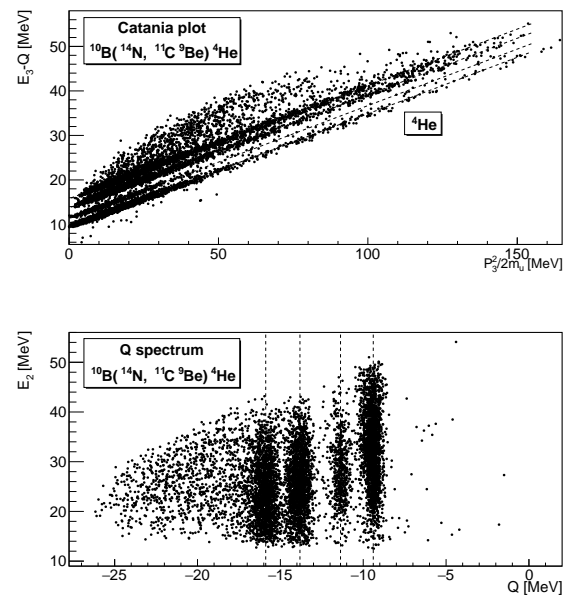
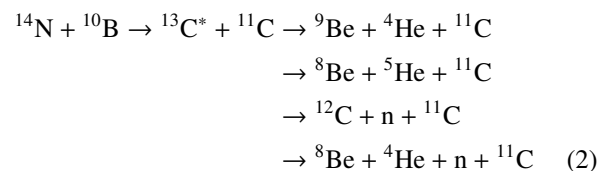


Figure 3: Catania plot (*top*) and Q -value spectrum (*bottom*) for the $^{10}\text{B}(^{14}\text{N}, ^{11}\text{C}^9\text{Be})^4\text{He}$ reaction. Four loci represent events with all products in their ground state (bottom and furthest right), ^{11}C excited to the 2.0 MeV ($1/2^-$) state (above ground state and left of the ground state), possible mixture of more than one state (remaining two).

With a cut at around 17 MeV, ^{15}O intermediate states were separated from ^{13}C states of interest.

As shown in the identification plots (Figure 2), a wide range of isotopes has been detected, allowing for the study of numerous cluster decays with $^{14}\text{N} + ^{10}\text{B}$ reaction. While the [31] gave an overview of both the ^{11}C and ^{13}C decays, this report will primarily focus on the ^{13}C isotope, with the following potential ^{13}C decay channels:



The collected data varied in statistical quality depending on the reaction exit channels and detection combinations, resulting in different binning resolutions ranging from 50 keV to 250 keV. Preliminary results presented in the following section will focus on the first listed decay channel, with further publications providing a more comprehensive analysis of the remaining decay channels.

3 Results

This section presents results for two reaction channels, involving two- and three-body reaction products. In the $^{10}\text{B}(^{14}\text{N}, ^{11}\text{C})^{13}\text{C}$ reaction, the ^{11}C nucleus was detected, and excitation energy of ^{13}C was determined using Equation 1. The presented results are for single events of the ^{11}C detection in one detector telescope. In Figure 4, excitation energy is plotted as a function of the detection angle. Since the excitation energy should remain constant with respect to the detection angle for a specific exit channel (with precise mass assignments), any bent locus in the plot indicates inaccuracies in the event reconstruction caused by uncertainties in detector geometry, energy calibration, energy loss calculations, or incorrect identification of reaction channels, potentially arising from target contaminants or misidentified detected reaction product. The projection of the 2D spectrum on the x-axis is also shown in Figure 4. A shift of approximately 400 keV of the ground state

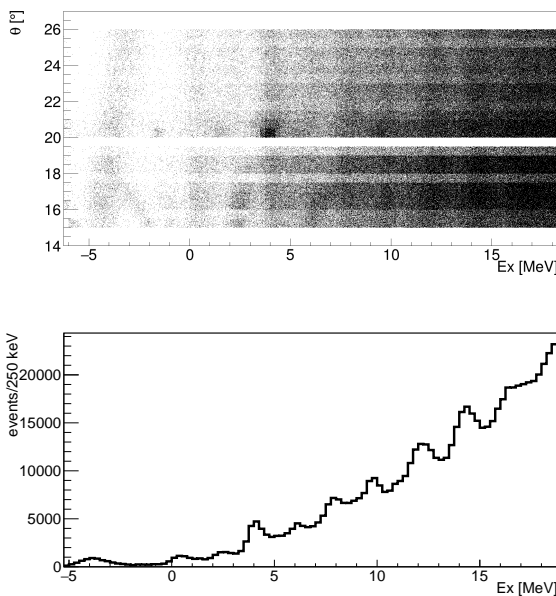


Figure 4: (top) The ^{13}C excitation energy from the $^{10}\text{B}(^{14}\text{N}, ^{11}\text{C})^{13}\text{C}$ reaction as a function of detection angle, with a projection of the spectrum on x-axis (bottom).

position is observed, indicating that all subsequent peaks must be adjusted by the same amount for accurate interpretation (this correction is applied in further text). There are nine potential state candidates, with the first four being clearly identifiable: the ground state, a peak at around 2.0 MeV corresponding to the first excited state of ^{11}C (2.0 MeV, $1/2^-$), a peak at 3.7 MeV likely corresponding to the

^{13}C 3.68 ($3/2^-$) state, and a peak at 5.7 MeV possibly indicating that both ^{11}C and ^{13}C were excited to 2.0 MeV and 3.7 MeV, respectively, as there is no known state at this energy. The remaining five states, located around 7.4, 9.4, 11.7, 13.9, and 15.9 MeV, require further investigation since there are possibilities for their interpretation, which will be addressed in future publications. For this analysis, a binning of 250 keV was used.

Reconstruction of the events with three decay products in the exit channel is more complex due to the sequential decay of one of the nuclei produced in the first step of the reaction process. Since decay thresholds are lying above the ground state, unlike in the case in Figure 4 clear reference for systematic shifts is not available. As a result, we rely on well-documented states in ^{13}C to accurately determine the energies of other states. However, in this case, no suitable reference state was found, so the focus shifted to a reaction channel similar to $^{10}\text{B}(^{14}\text{N}, ^{11}\text{C}^9\text{Be})^4\text{He}$. Given that energy shifts result primarily from uncertainties in energy-loss corrections and detector geometry, affecting both calibration and event reconstruction, particles with comparable masses and detection energies (and positions) should exhibit similar shifts. Therefore, we first examined the $^{10}\text{B}(^{14}\text{N}, ^{12}\text{C}^8\text{Be})^4\text{He}$ reaction. Figure 5 presents a correlation plot between the excitation energies of different intermediate states, along with the excitation spectrum of ^{12}C , where the red curve represents detection efficiency obtained by detailed Monte Carlo simulations of the reaction process and experimental setup. Three peaks

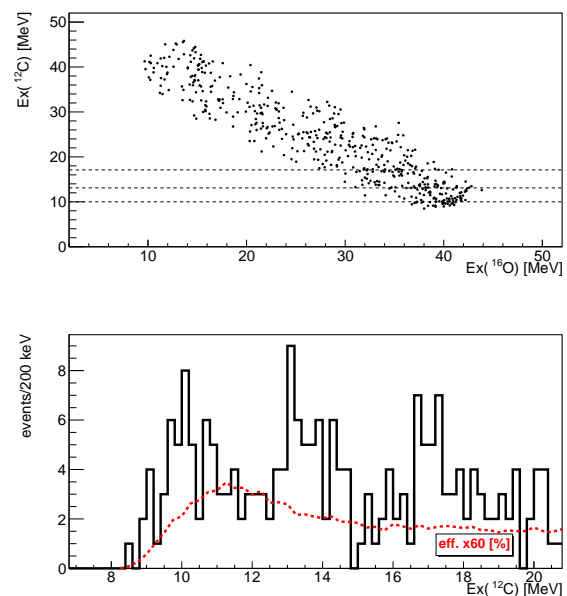


Figure 5: (top) Correlation plot for the excitation energies of ^{12}C and ^{16}O with horizontal lines representing the states in ^{12}C ; (bottom) Excitation-energy spectrum for the decays of the ^{12}C excited states to $^8\text{Be}_{gs}$ and $^4\text{He}_{gs}$.

are observed in both plots, with dashed lines indicating states around 10.0 MeV, 13.1 MeV, and 17.1 MeV. After accounting for experimental resolution and a systematic shift of approximately 350 keV, these peaks could corre-

spond to known states at 9.64 (3^-), and 12.71 (1^+), while the third state remains under discussion.

The decay of ^{13}C to ^9Be and ^4He was examined using the $^{10}\text{B}(^{14}\text{N}, ^{11}\text{C})^9\text{Be}^4\text{He}$ reaction channel. Here, the ^{11}C and ^9Be nuclei were detected on opposite sides of the beamline. Figure 6 shows the correlation plots between the excitation energies of different product combinations. A vertical dashed line indicates where a cut was made to

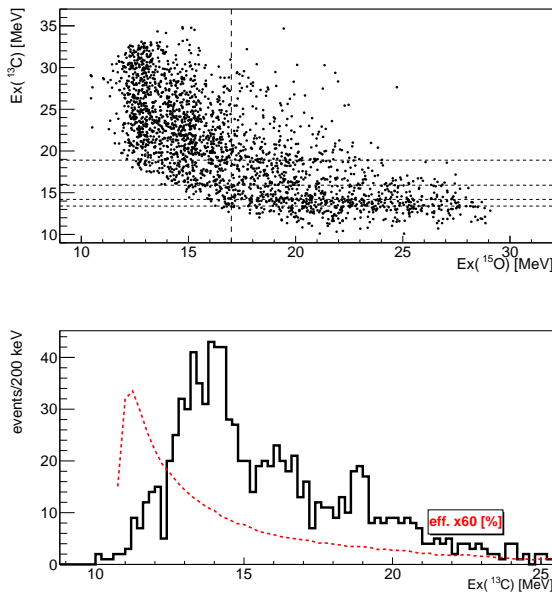


Figure 6: (top) Correlation plot for the excitation energies of ^{13}C and ^{15}O with vertical line representing separation at ≈ 17 MeV of ^{15}O intermediate states and horizontal lines representing the states in ^{13}C ; (bottom) Excitation-energy spectrum for the decays of the ^{13}C excited states to $^9\text{Be}_{gs}$ and $^4\text{He}_{gs}$.

isolate intermediate states of ^{15}O , while horizontal dashed lines represent candidates for states in ^{13}C . In the same figure, the excitation spectrum is presented with the detection efficiency curve. Several peaks are observed, indicating potential ^{13}C states undergoing alpha decay and exhibiting a cluster structure. Given the efficiency curve's maximum at lower energies, the first peak around 11.8 MeV is likely an artifact and has been excluded as a potential state. Between 13 and 14 MeV, a broad peak suggests the presence of two states at around 13.4 and 14.2 MeV, which, after applying a 350 keV shift, correspond to 13.1 and 13.9 MeV. A broader structure around 15.6 MeV (accounting for the shift) suggests the possibility of more states. Finally, a well-defined peak at 18.5 MeV is observed in both the correlation and excitation energy plots. Obtained results are consistent with previously published results [17, 18].

4 Conclusion

This report presents the preliminary results from the $^{14}\text{N}+^{10}\text{B}$ experiment, which aims to explore the cluster structure of various carbon isotopes. The experimental setup and analysis procedure for reactions involving

two and three products in the exit channels were outlined. Particular emphasis was placed on the excited states of ^{13}C observed through the $^{10}\text{B}(^{14}\text{N}, ^{11}\text{C})^{13}\text{C}$ and $^{10}\text{B}(^{14}\text{N}, ^{11}\text{C})^9\text{Be}^4\text{He}$ reactions. The obtained results are consistent with previously published results.

In the $^{10}\text{B}(^{14}\text{N}, ^{11}\text{C})^{13}\text{C}$ reaction channel, excited states were identified at 2.0, 3.7, 5.7, 7.4, 9.4, 11.7, 13.9, and 15.9 MeV. While the first three states are well understood, the remaining states will require more detailed investigation to fully interpret their significance for the clustering in ^{13}C . The $^{10}\text{B}(^{14}\text{N}, ^{11}\text{C})^9\text{Be}^4\text{He}$ exit channel revealed states at 13.1, 13.9, 15.6, and 18.5 MeV. A comprehensive interpretation of these results, along with a discussion of other exit channels referenced in Equation 2, will be provided in forthcoming publications.

References

- [1] A. Tohsaki, H. Horiuchi, P. Schuck, G. Röpke, Alpha cluster condensation in ^{12}C and ^{16}O , Phys. Rev. Lett. **87**, 192501 (2001). [10.1103/PhysRevLett.87.192501](https://doi.org/10.1103/PhysRevLett.87.192501)
- [2] Y. Funaki, A. Tohsaki, H. Horiuchi, P. Schuck, G. Röpke, Analysis of previous microscopic calculations for the second 0^+ state in ^{12}C in terms of $3-\alpha$ particle bose-condensed state, Phys. Rev. C **67**, 051306 (2003). [10.1103/PhysRevC.67.051306](https://doi.org/10.1103/PhysRevC.67.051306)
- [3] M. Chernykh, H. Feldmeier, T. Neff, P. von Neumann-Cosel, A. Richter, Structure of the hoyle state in ^{12}C , Phys. Rev. Lett. **98**, 032501 (2007). [10.1103/PhysRevLett.98.032501](https://doi.org/10.1103/PhysRevLett.98.032501)
- [4] Y. Funaki, Hoyle band and α condensation in ^{12}C , Phys. Rev. C **92**, 021302 (2015). [10.1103/PhysRevC.92.021302](https://doi.org/10.1103/PhysRevC.92.021302)
- [5] A. Raduta, B. Borderie, E. Geraci, N. Le Neindre, P. Napolitani, M. Rivet, R. Alba, F. Amorini, G. Cardella, M. Chatterjee et al., Evidence for α -particle condensation in nuclei from the hoyle state deexcitation, Physics Letters B **705**, 65 (2011). <https://doi.org/10.1016/j.physletb.2011.10.008>
- [6] Y. Kanada-En'yo, Variation after angular momentum projection for the study of excited states based on antisymmetrized molecular dynamics, Phys. Rev. Lett. **81**, 5291 (1998). [10.1103/PhysRevLett.81.5291](https://doi.org/10.1103/PhysRevLett.81.5291)
- [7] T. Suhara, Y. Funaki, B. Zhou, H. Horiuchi, A. Tohsaki, One-dimensional α condensation of α -linear-chain states in ^{12}C and ^{16}O , Phys. Rev. Lett. **112**, 062501 (2014). [10.1103/PhysRevLett.112.062501](https://doi.org/10.1103/PhysRevLett.112.062501)
- [8] Y. Chiba, M. Kimura, Hoyle-analog state in ^{13}C studied with antisymmetrized molecular dynamics, Phys. Rev. C **101**, 024317 (2020). [10.1103/PhysRevC.101.024317](https://doi.org/10.1103/PhysRevC.101.024317)
- [9] N. Furutachi, M. Kimura, Bent three- α linear-chain structure of ^{13}C , Phys. Rev. C **83**, 021303 (2011). [10.1103/PhysRevC.83.021303](https://doi.org/10.1103/PhysRevC.83.021303)
- [10] T. Yamada, Y. Funaki, α -cluster structures and monopole excitations in ^{13}C , Phys. Rev. C **92**, 034326 (2015). [10.1103/PhysRevC.92.034326](https://doi.org/10.1103/PhysRevC.92.034326)

- [11] N. Itagaki, W.v. Oertzen, S. Okabe, Linear-chain structure of three α clusters in ^{13}C , *Phys. Rev. C* **74**, 067304 (2006). [10.1103/PhysRevC.74.067304](https://doi.org/10.1103/PhysRevC.74.067304)
- [12] M. Freer, E. Casarejos, L. Achouri, C. Angulo, N.I. Ashwood, N. Curtis, P. Demaret, C. Harlin, B. Laurent, M. Milin et al., $\alpha:2n:\alpha$ molecular band in ^{10}Be , *Phys. Rev. Lett.* **96**, 042501 (2006). [10.1103/PhysRevLett.96.042501](https://doi.org/10.1103/PhysRevLett.96.042501)
- [13] M. Milin, M. Zadro, S. Cherubini, T. Davinson, A. Di Pietro, P. Figuera, Đ. Miljanić, A. Musumarra, A. Ninane, A. Ostrowski et al., Sequential decay reactions induced by a 18 MeV ^6He beam on ^6Li and ^7Li , *Nuclear Physics A* **753**, 263 (2005). <https://doi.org/10.1016/j.nuclphysa.2005.02.154>
- [14] N. Soić, S. Blagus, M. Bogovac, S. Fazinić, M. Lattuada, M. Milin, D. Miljanić, D. Rendić, C. Spitaleri, T. Tadić et al., $^6\text{He} + \alpha$ clustering in ^{10}Be , *Europhysics Letters* **34**, 7 (1996). [10.1209/epl/i1996-00407-y](https://doi.org/10.1209/epl/i1996-00407-y)
- [15] N. Vukman, N. Soić, M. Freer, M. Alcorta, D. Connolly, P. Čolović, T. Davinson, A. Di Pietro, A. Lennarz, A. Psaltis et al., Cluster decays of ^{12}Be excited states, *Frontiers in Physics* **10** (2022). [10.3389/fphy.2022.1009421](https://doi.org/10.3389/fphy.2022.1009421)
- [16] M. Milin, W. von Oertzen, Search for molecular bands in ^{13}C , *The European Physical Journal A - Hadrons and Nuclei* **14**, 295 (2002). [10.1140/epja/i2001-10199-6](https://doi.org/10.1140/epja/i2001-10199-6)
- [17] I. Lombardo, D. Dell'Aquila, G. Spadaccini, G. Verde, M. Vigilante, Spectroscopy of ^{13}C above the α threshold with $\alpha + ^9\text{Be}$ reactions at low energies, *Phys. Rev. C* **97**, 034320 (2018). [10.1103/PhysRevC.97.034320](https://doi.org/10.1103/PhysRevC.97.034320)
- [18] M. Freer, N.I. Ashwood, N. Curtis, A. Di Pietro, P. Figuera, M. Fisichella, L. Grassi, D. Jelavić Malenica, T. Kokalova, M. Koncul et al., Analysis of states in ^{13}C populated in $^9\text{Be} + ^4\text{He}$ resonant scattering, *Phys. Rev. C* **84**, 034317 (2011). [10.1103/PhysRevC.84.034317](https://doi.org/10.1103/PhysRevC.84.034317)
- [19] N. Soić, M. Freer, L. Donadille, N.M. Clarke, P.J. Leask, W.N. Catford, K.L. Jones, D. Mahboub, B.R. Fulton, B.J. Greenhalgh et al., Three-centre cluster structure in 11c and 11b, *Journal of Physics G: Nuclear and Particle Physics* **31**, S1701 (2005). [10.1088/0954-3899/31/10/057](https://doi.org/10.1088/0954-3899/31/10/057)
- [20] D. Price, M. Freer, S. Ahmed, N. Ashwood, N. Clarke, N. Curtis, P. McEwan, C. Metelko, B. Novatski, S. Sakuta et al., Alpha-decay of excited states in ^{13}C and ^{14}C , *Nuclear Physics A* **765**, 263 (2006). <https://doi.org/10.1016/j.nuclphysa.2005.11.004>
- [21] D. Jelavić Malenica, M. Milin, D. Dell'Aquila, A. Di Pietro, P. Figuera, I. Gašparić, T. Mijatović, A. Musumarra, M.G. Pellegriti, V. Scuderi et al., The ^{13}C states populated in $^{10}\text{B} + ^{10}\text{B}$ reactions at 72 MeV, *The European Physical Journal A* **59**, 228 (2023).
- [22] N. Soić, M. Freer, L. Donadille, N. Clarke, P. Leask, W. Catford, K. Jones, D. Mahboub, B. Fulton, B. Greenhalgh et al., Cluster structure of ^{13}C probed via the $^7\text{Li}(^9\text{Be}, ^{13}\text{C}^* \rightarrow ^9\text{Be} + \alpha)$ reaction, *Nuclear Physics A* **728**, 12 (2003). <https://doi.org/10.1016/j.nuclphysa.2003.08.029>
- [23] C. Wheldon, N.I. Ashwood, M. Barr, N. Curtis, M. Freer, T. Kokalova, J.D. Malcolm, V.A. Ziman, T. Faestermann, H.F. Wirth et al., Absolute partial decay-branch measurements in ^{13}C , *Phys. Rev. C* **86**, 044328 (2012). [10.1103/PhysRevC.86.044328](https://doi.org/10.1103/PhysRevC.86.044328)
- [24] A.S. Demyanova, A.N. Danilov, S.V. Dmitriev, A.A. Ogloblin, V.I. Starastin, S.A. Goncharov, D.M. Jansetov, Search for Exotic States in ^{13}C , *JETP Letters* **114**, 303 (2021). [10.1134/S0021364021180016](https://doi.org/10.1134/S0021364021180016)
- [25] K. Inaba, Y. Sasamoto, T. Kawabata, M. Fujiwara, Y. Funaki, K. Hatanaka, K. Itoh, M. Itoh, K. Kawase, H. Matsubara et al., Search for α condensed states in ^{13}C using α inelastic scattering, *Progress of Theoretical and Experimental Physics* **2021**, 093D01 (2021). [10.1093/ptep/ptab102](https://doi.org/10.1093/ptep/ptab102)
- [26] D. Jelavić Malenica, M. Milin, S. Blagus, A. Di Pietro, P. Figuera, M. Lattuada, Đ. Miljanić, A. Musumarra, M.G. Pellegriti, L. Prepolec et al., ^{12}C states populated in $^{10}\text{B} + ^{10}\text{B}$ reactions, *Phys. Rev. C* **99**, 064318 (2019). [10.1103/PhysRevC.99.064318](https://doi.org/10.1103/PhysRevC.99.064318)
- [27] C. Wheldon, T. Kokalova, M. Freer, A. Glenn, D.J. Parker, T. Roberts, I. Walmsley, States at high excitation in ^{12}C from the $^{12}\text{C}(^3\text{He}, ^3\text{He})3\alpha$ reaction, *Phys. Rev. C* **90**, 014319 (2014). [10.1103/PhysRevC.90.014319](https://doi.org/10.1103/PhysRevC.90.014319)
- [28] L. Tassan-Got, A new functional for charge and mass identification in $\Delta E-E$ telescopes, *Nuclear Instruments and Methods in Physics Research Section B: Beam Interactions with Materials and Atoms* **194** (2001). [10.1016/S0168-583X\(02\)00957-6](https://doi.org/10.1016/S0168-583X(02)00957-6)
- [29] N. Le Neindre, M. Alderighi, A. Anzalone, R. Barnà, M. Bartolucci, I. Berceanu, B. Borderie, R. Bougault, M. Bruno, G. Cardella et al., Mass and charge identification of fragments detected with the chimera silicon-csi(tl) telescopes, *Nuclear Instruments and Methods in Physics Research Section A: Accelerators, Spectrometers, Detectors and Associated Equipment* **490**, 251 (2002). [https://doi.org/10.1016/S0168-9002\(02\)01008-2](https://doi.org/10.1016/S0168-9002(02)01008-2)
- [30] E. Costanzo, M. Lattuada, S. Romano, D. Vinciguerra, M. Zadro, A procedure for the analysis of the data of a three body nuclear reaction, *Nuclear Instruments and Methods in Physics Research Section A: Accelerators, Spectrometers, Detectors and Associated Equipment* **295**, 373 (1990). [https://doi.org/10.1016/0168-9002\(90\)90715-I](https://doi.org/10.1016/0168-9002(90)90715-I)
- [31] L. Palada et al., Clustering in $^{11,12,13}\text{C}$, *Acta Phys. Pol. B Proc. Suppl.* **17**, 3 (2024). <https://doi.org/10.5506/APhysPolBSupp.17.3-A31>